AUTOMATED KAGUYA TC AND MRO CTX DIGITAL ELEVATION MODEL GENERATION WITH AMES STEREO PIPELINE. L. A. Adoram-Kershner[1], B. H Wheeler[1], J. R. Laura[1], R. L. Fergason[1], and D. P. Mayer[1], [1]USGS, Astrogeology Science Center, 2255 N. Gemini Dr., Flagstaff, AZ, 86001; ladoram-kershner@usgs.gov.

Introduction: The Planetary Spatial Data Infrastructure (PSDI) [1,2] describes Digital Elevation Models (DEMs) as foundational products because, with the proper resolution and accuracy, they can support many planetary science or engineering studies [e.g., 3,4]. The resolution and accuracy needed for the DEM is determined by the study's requirements. For example, the Mars 2020 Jezero crater landing site analysis required high fidelity DEMs with resolution and accuracy in the low single meter range [5]. Other studies, such as change detection focused studies (e.g., sediment tracking) can use DEMs with lower resolution and accuracy. Currently, most publicly available DEMs are produced manually using proprietary software, such as SOCET SET® or SOCET GXP®, to achieve highly accurate products. The time and expertise required to create quality DEMs coupled with the high acquisition rates of images from planetary missions has resulted in a high potential between available stereographic images and corresponding DEM products. Additionally, the time and specialized staff required for traditional DEM production can also be a barrier for projects without adequate funding to cover traditional DEM generation. Herein, we outline an automated DEM generation pipeline which leverages open-source software, including the USGS Integrated Software for Imagers and Spectrometers (ISIS) [6] and the NASA Ames Stereo Pipeline (ASP) [7]. The pipeline starts with raw image data then calibrates the data and generates DEMs through stereogrammetry, requiring minimal human involvement. The pipeline is applied to the Mars Reconnaissance Orbiter Context Camera (CTX) [8] and the Kaguya Terrain Camera (KTC) [9] data, which is then evaluated. This work builds on previous research conducted by Mayer et al. [10,11] and the initial work on this pipeline is described in [12].

Image Preprocessing: The pipeline begins with raw image data, so DEMs can be generated using the most recent calibration and processing algorithms from the mission teams. Initial image processing uses ISIS ingestion (*mroctx2isis* or *kagtc2isis*), *spiceinit*, and the available mission specific ISIS commands. For CTX these mission specific commands include *ctxcal* and *ctxevenodd* (as needed). KTC has no mission specific calibration commands in ISIS as of version 4.4.0.

Relative Alignment: Once the ISIS cubes are ingested and preprocessed, ASP's *bundle_adjust* is used to relatively align the stereo images through camera orientation adjustments. Having self-consistent stereo image cameras reduces the relative errors and uncertainties in the final DEM and is a standard process before attempting DEM generation. The pipeline *bundle_adjust* uses Optimized Box Approximation of Laplacian of Gaussian (OBA-LoG) detectors and reruns with scale-invariant feature transform (SIFT) detectors if camera adjustments were not successfully generated.

DEM Generation: In our pipeline, we run ASP's *stereo* program two times, in sequence. The program is first run on the bundle-adjusted images, and the resulting point cloud is used to create an initial, low-resolution DEM. We then project the bundle-adjusted images onto this initial DEM to reduce the long-wavelength disparity between the images. The projected images are then input to a second run of *stereo* and the resulting point cloud is aligned to ground and used to generate the final DEM.

Initial DEM: The initial DEM is generated by running the bundle-adjusted cubes through ASP's *stereo* and *point2dem* functions. The pipeline applies *stereo* preprocessing (*stereo_pprc*), disparity map initialization (*stereo_corr*), subpixel refinement (*stereo_rfne*), outlier rejection and hole filling (*stereo_fltr*), and triangulation (*stereo_tri*) steps. The output of *stereo* is a 3D point cloud representing the successfully triangulated positions between the stereographic images, and *point2dem* ingests this point cloud and outputs a DEM with user defined post-spacing. Since this DEM is not the final product but a projection surface for the bundle-adjusted cubes, the post-spacing value was set to 100 m (much greater than the 10 m/pixel KTC resolution and 7 m/pixel CTX resolution).

Positions that were not successfully triangulated by stereo will not be output into the DEM, leaving blank pixels, or "holes." Any holes present in the initial DEM will propagate, with increasing size, to the projected cubes and the full-resolution DEM. To avoid holes in the initial DEM, *point2dem* is run with the *--dem-hole-fill-len* parameter set. The bundle-adjusted images are then projected onto this DEM.

Final DEM: The final DEM is generated by running the projected bundle-adjusted images through *stereo*, aligning the resulting point cloud to ground altimetry measurements (see Ground Sources section for details on ground data used) using ASP's *pc_align*, and then running *point2dem* on the aligned point cloud.

The pipeline runs the same *stereo* steps from the initial DEM generation, but with different

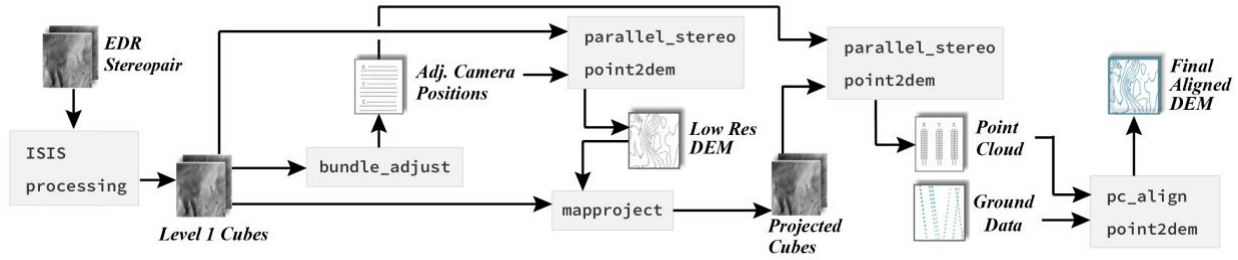

***Figure 1**: Flowchart of the DEM Pipeline. Specific ISIS processing commands for KTC and CTX are described in "Image Preprocessing." The altimetry ground data used for KTC and CTX point cloud alignment is described in the "Ground Sources."*

parameterization. To align the resulting point cloud to ground the pipeline leverages two of the available *pc_align* algorithms; the Iterative Closest Point (ICP) and Fast Global Registration (FGR) algorithms. FGR is more accurate than ICP when the clouds are nearly aligned and is more robust to outliers, while ICP is more robust to larger initial offsets. So, *pc_align* is run using ICP first, following the method outlined in [12], and a second *pc_align* is run using FGR and pre-applying the ICP transformation (with *--initial-transform* flag).

The post-spacing for the final *point2dem* call is 35 m for KTC and 21 m for CTX. These values are equal to approximately three times the average original data resolution (10 m/pixel for KTC and 7 m/pixel for CTX) which is the expected maximum resolution for stereogrammetically derived DEMs [13]. A flowchart of the entire pipeline process is displayed in Figure 1.

Ground Sources: The accepted geodetic reference frame for Mars is the Mars Orbiter Laser Altimeter (MOLA) [14] data set. The accepted geodetic reference frame for the Moon is Lunar Orbiter Laser Altimeter (LOLA) obtained from the Orbital Data Explorer (ODE) [15]. In both cases, the ground source data are being queried with a tight footprint and only includes ground points within the DEM footprint.

Validation: Validation of the original pipeline, which consisted of comparisons between pipeline DEMs and benchmark DEMs, is described in [12]. Alterations have been made to the pipeline since this validation, but initial tests show the DEM elevations are in line with previously generated DEMs, suggesting the pipeline is performing well. The presentation associated with this abstract will fully describe the results of the updated pipeline's validation.

Data Serving: The usefulness of these products is dependent on their discoverability, interoperability, and reproducibility as described by the FAIR guiding principles framework [16]. To that end, we are serving the DEMs and their associated orthoimages as analysis ready data (ARD), using the spatio-temporal asset catalog (STAC) [17]. These data are served as cloud optimized GeoTIFFs (COGs) which are analysis and GIS ready without additional processing. We also serve FGDC compliant metadata [18] and provenance files (a history of processing steps used to produce the DEMs) to further improve reproducibility. After validation, we will make all data publicly available via Amazon Web Service (AWS) S3 buckets.

Acknowledgments: The MRO CTX data were provided by the PDS Cartography and Imaging Sciences Node. The MOLA and LOLA data were provided by the PDS Geosciences Node. Kaguya TC data and support were provided by the SELENE team and Data Archive operated by JAXA. Any use of trade, firm, or product names is for descriptive purposes only and does not imply endorsement by the U.S. Government.

References: [1] Gaddis L. (2018) *LPSC XLIX*, 2081 or 1540. [2] Laura J. R., et al. (2017) *ISPRS International Journal of Geo-Information* 6.6, 181. [3] Kirk, R. L., et al. (2008) J. Geophys. Res., 113, E00A24, doi:10.1029/2007 JE003000. [4] Xiong, S., et al. (2021) *Earth and Space Science*, 8(1), e2019EA000968. [5] Galuszka, D., et al. (2020) *LPSC LI*, Abstract No. 2020. [6] USGS Astrogeology (2020) https://doi.org/10.5281/zenodo.3962369. [7] Beyer, R., et al. (2020) https://doi.org/10.5281/zenodo.396334. [8] Malin, M. C., et al. (2007) *J. Geophys. Res.*, 112, E05S04, doi:10.1029/2006JE002808. [9] Haruyama, J., Matsunaga, T., Ohtake, M. et al. (2008) *Earth Planet Space* 60, 243–255, doi:10.1186/BF03352788. [10] Mayer, D.P. and Kite, E.S. (2016) *LPS XLVII*, ePosterAbstract No. 1241. [11] Mayer, D.P. (2018) *LPSC XLIX*, Abstract No. 1604. [12] Adoram-Kershner, L.A., et al. (2021) *Planetary Data & PSDIA V*, Abstract No. 7021. [13] Kirk, R.L., et al. (2021) Remote Sensing, 13(17), 3511, doi:10.3390/rs13173511. [14] Neumann, G. A, et al. (2001) *J. Geophys. Res.*, 106, 23,753–23,768. [15] Smith, D. E., et al. (2008) *Eos Trans. AGU*, 87 (52), U41C –0826. [16] GO FAIR. (2021). Fair principles. GO FAIR. Retrieved from https://www.go-fair.org/fair-principles/ [17] SpatioTemporal Asset Catalog. (2019) *SpatioTemporal Asset Catalog*, [Online] https://radiantearth. github.io/stac-site/. [18] Federal Geographic Data Committee. (1998) *Federal Geographic Data Committee*, FGDC-STD-001-1998.